Glacial lake inventory of High Mountain Asia in 1990 and 2018 derived from Landsat images

Xin Wang [1,2], Xiaoyu Guo [1], Chengde Yang [2], Qionghuan Liu [3], Junfeng Wei [1], Yong Zhang [1],
Shiyin Liu [4], Yanlin Zhang [1], Zongli Jiang [1], Zhiguang Tang [1]

[1]School of Resource Environment and Safety Engineering, Hunan University of Science and Technology, Xiangtan, 411100, China
[2]State Key Laboratory of Cryospheric Science, Northwest Institute of Ecology and Environmental Resources, Chinese Academy of Sciences, Lanzhou 730000, China
[3]Key Laboratory of Land Surface Pattern and Simulation, Institute of Geographic Sciences and Natural Resources Research, Chinese Academy of Sciences, Beijing 100101, China
[4]Institute of International Rivers and Eco-security, Yunnan University, Kunming, 650000 China

Correspondence to: Xin Wang (xinwang_hn@163.com)

Abstract. There is currently no glacial lake inventory data set for the entire High Mountain Asia (HMA) area. The definition and classification of glacial lakes remain controversial, presenting certain obstacles to extensive utilization of glacial lake inventory data. This study integrated glacier inventory data and 668 Landsat TM/ETM+/OLI images, and adopted manual visual interpretation to extract glacial lake boundaries within a 10-km buffer from glacier extent using ArcGIS and ENVI software, normalized difference water index maps, and Google Earth images. The theoretical and methodological basis for all processing steps including glacial lake definition and classification, lake boundary delineation, and uncertainty assessment are discussed comprehensively in the paper. Moreover, detailed information regarding the coding, location, perimeter and area, area error, type, time phase, source image information, and sub-regions of the located lakes is presented. It was established that 27,205 and 30,121 glacial lakes (size: 0.0054–6.46 km^2) in HMA, covered a combined area of 1806.47 ± 2.11and 2080.12 ± 2.28 km^2 in 1990 and 2018, respectively. The data set is now available from the National Special Environment and Function of Observation and Research Stations Shared Service Platform (China): http://www.crensed.ac.cn/portal/metadata/706ce17f-1684-4e8d-bf5e-7d517e03693c

1 Introduction

Under the background of climate warming and the consequent widespread mass loss of glaciers in alpine regions, increasing volumes of glacial meltwater are being released. This results in glacial lake expansion and extended areas of low-lying terrain (e.g., depressions and troughs) left behind by

retreating glaciers in which water can accumulate and new glacial lakes can form (Clague and Evans, 2000; Mool et al., 2001; Song et al., 2016). As both a water resource and a source of flash flood/debris flow hazards, glacial lakes participate in several natural processes, e.g., regional energy and water cycles (Slemmons et al., 2013), act as both indicators and containers of environmental information (Wang et al., 2016, 2019b; Zhang et al., 2019), and drive hillslope erosion and landscape evolution (Cook et al., 2018) in the alpine cryosphere. On the one hand, glacial lakes act as temporary storage for the meltwater resource because a considerable amount of meltwater is retained by glacial lake expansion, e.g., approximately 0.2 % a^{-1} of the total glacial meltwater was reserved in glacial lakes from 1990 to 2010 in the Tien Shan Mountains in Central Asia (Wang et al., 2013). On the other hand, given the worldwide expansion in lake area in recent decades, the potential will increase for glacial lakes to develop into glacial lake outburst floods and related debris flows that could threaten downstream residents, infrastructure, and regional ecological and environmental security (Huggel et al., 2002; ICMOD, 2011; Bolch et al., 2012; Haebeli et al., 2016). Thus, glacial lakes perform important roles both in the meltwater cycle and in glacier hazard evolution in the cryosphere.

Following the rapid development of remote sensing technology and computer science, remote sensing imagery acquired by various satellites and sensors has been used widely in glacial lake research. In particular, Landsat imagery has become the most important data source for dynamic investigation of glacial lakes because of its wide coverage, continuous and long-term temporal sequence, and accessibility. Based on remote sensing data, both the distribution and the characteristics of change of glacial lakes in the mountains and watersheds in the High Mountain Asia (HMA) region have been widely reported (Supplementary Table S1). For example, multi-source remote sensing imagery has been used to compile glacial lake inventories for regions of the Tibetan Plateau (Zhang et al., 2015), Tien Shan Mountains (Wang et al., 2013), Himalaya (Gardelle et al., 2011; Nie et al., 2017), Hengduan Mountains (Wang et al., 2017), Uzbekistan (Petrov et al., 2017), Pakistan (Senese et al., 2018), and HMA, excluding Altay and Sayan (Chen et al., 2020). These inventories have proved an important data resource both for revealing the spatiotemporal characteristics of glacial lakes and for understanding the response of glacial lakes to the effects of climate change in these regions.

Automatic and semi-automatic glacial lake boundary vectorization approaches have been used most widely in regional glacial lake investigations because of their higher efficiency and objectivity in comparison with manual visual vectorization. In such research, water bodies are usually determined based on the characteristics of different remote sensing bands and computer-dependent algorithms, e.g.,

the normalized difference water index (NDWI), band ratio, support vector machine, decision tree, spectral transformation, object-oriented classification, global-–local iterative scheme, active contour model, and random forest (Gardelle et al., 2011–; Huggel et al., 2002–; Li et al., 2011; Veh et al., 2018–; Zhang et al., 2018). However, manual post-processing is often required to calibrate the uncertainties that could easily be produced by the above approaches. Furthermore, the labour costs associated with rectification of lake boundary errors increase sharply with increasing complexity of study area terrain (Yang et al., 2019). With consideration of the accuracy, efficiency, and time overheads associated with the various vectorization approaches, a manual vectorization approach was adopted for investigation of the glacial lakes on the Tibetan Plateau (Zhang et al., 2015) despite the labour requirements and the anticipated additional errors produced by individual subjectivity (Nie et al., 2017; Yang et al., 2019; Song et al., 2014).

Controversies and knowledge gaps remain regarding available glacial lake inventories for different alpine cryosphere regions, which present certain obstacles to extensive utilization of glacial lake inventory data. The main problems relate to regional differences in lake development, inconsistent specifications of lake definition, and the adoption of various approaches regarding lake interpretation (Yao et al., 2018). There is no existing comprehensive glacial lake inventory for the entire HMA and knowledge regarding the spatiotemporal characteristics of glacial lakes in this region remains incomplete. The objectives of this study were to fill this knowledge gap by producing a glacial lake inventory data set for HMA derived from Landsat images, and to provide fundamental data for water resource evaluation, assessment of glacial lake outburst floods, and glacier hydrology research in the mountain cryosphere region.

2 Study area

The HMA area mainly comprises the Tibetan Plateau and surrounding alpine ranges. The area is divided into 13 sub-regions in version 5–6 of the Randolph Glacier Inventory (RGI 6.0), i.e., the Himalaya area (Western Himalaya, Central Himalaya, and Eastern Himalaya), Hengduan Mountains, Southern and Eastern Tibet, Inner Tibetan Plateau, Karakoram and Western Kun Lun, Qilian Shan and Eastern Kun Lun, Hindu Kush, Pamir, Hissar Alay and Western Tien Shan, Eastern Tien Shan, and Altay and Sayan (Arendt et al., 2015; Pfeffer et al., 2014). The boundaries of the 13 sub-regions and outlines of the glaciers in HMA derived from RGI 6.0 are shown in Figure 1. This region (26°–54°N, 67°–104°E) is characterized by tremendously complex topographic conditions with widespread distribution of mountain glaciers. According to the Climatic Research Unit Time Series v4.02 data set

1 (http://data.ceda.ac.uk/badc/cru/data/cru_ts/cru_ts_4.02/), the air temperature of the different

2 sub-regions in HMA increased at an average annual rate of 0.002–0.054 °C a^{-1} during 1990–2018 (Fig.

3 1). The annual rate of change of precipitation in HMA during 1990–2018 varied from −9.9 to 4.2 mm

4 a^{-1} with a small average rate of increase of 0.3 mm a^{-1}.
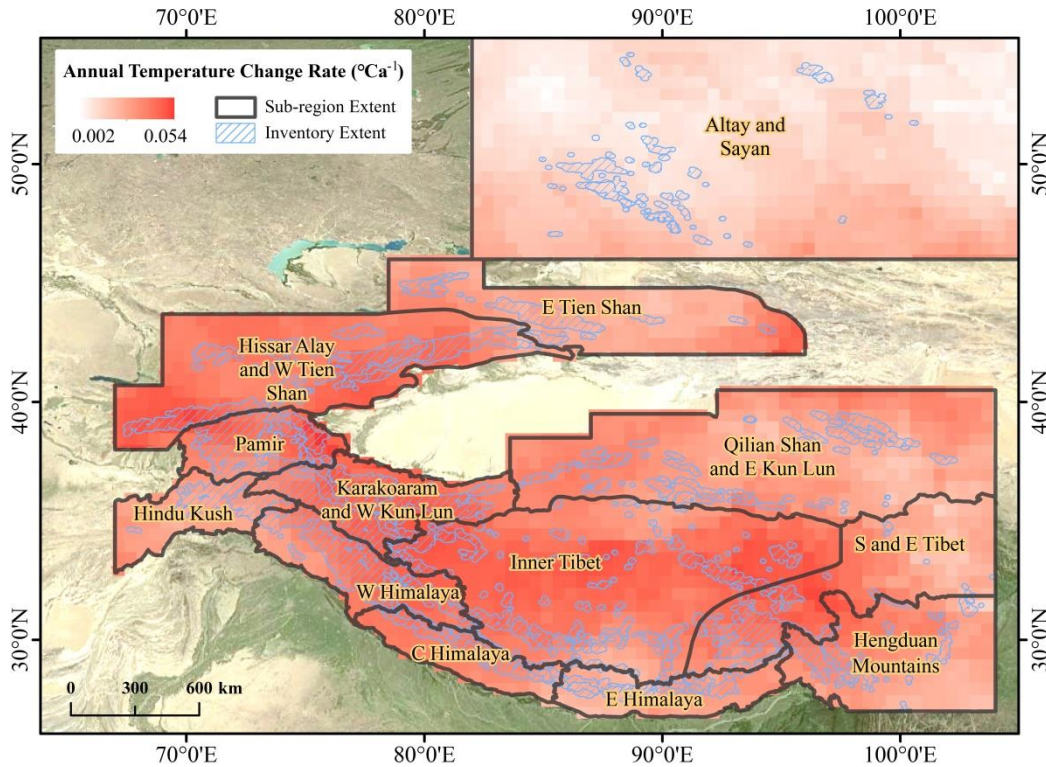
6 Figure 1. Location of sub-regions, rate of change of air temperature (1990–2018), and buffer area within

7 10 km of glacier extent for glacial lake inventory of High Mountain Asia.

8   The HMA area has the largest surviving glaciers of any region other than the polar regions. As

9 reported in RGI 6.0, there were 97,974 modern glaciers in our study area, covering a total area of

10 approximately 98,768.86 km^2. Together, these glaciers produced an average negative mass balance of

11 −150 ± 110 kg m^{-2} a^{-1} (Hock, et al., 2019)–, which was the primary source of water supply for the

12 development of glacial lakes. Over recent decades, glaciers in most areas of HMA appear to have

13 experienced widespread mass wastage and area shrinkage (Bolch et al., 2012; Yao et al., 2012; Kääb et

al., 2012; Brun et al., 2017). However, the so-called "Karakoram Anomaly" refers to a region that is a prominent exception, which is characterized by glaciers with stable or positive mass balance (Hewitt, 2005; Gardner et al., 2013; Kääb et al., 2015).

3 Data source

We developed our glacial lake inventory of HMA based on 668 high-quality images selected from more than 1800 Landsat images with 30-m spatial resolution derived from the websites of the United States Geological Survey (https://www.usgs.gov/) and Geospatial Data Cloud (http://www.gscloud.cn/). To ensure the accuracy of glacial lake boundary extraction, the following criteria were applied to imagery selection. First, the cloud coverage in an image had to be <10 %. Second, for areas with no eligible or only low-quality imagery (because of snow or shadows) in the given year, acceptable images from years closest to the given year were chosen as replacements (Fig. 2). Third, images acquired in summer or autumn (June–November), when lake areas were believed near or at their maximal extent, were set as optimal choices to minimize the impact produced by seasonal area changes of the glacial lakes (Fig. 2). Based on the above criteria, 394 and 274 Landsat images were selected to represent circa 1990 and circa 2018, respectively, which completely covered the buffer area within 10 km of glacier extent acquired from the Second Chinese Glacier Inventory (http://westdc.westgis.ac.cn) and RGI 6.0 (https://www.glims.org/RGI/rgi60_dl.html). Among the selected images, those acquired during summer and autumn (June–November) accounted for 82.0 % of the total number of selected images, while those acquired during autumn (September–November) accounted for 56.9 % of the total number. In addition, a Shuttle Radar Topography Mission digital elevation model with spatial resolution of 1″ (http://imagico.de/map/demsearch.php) was used to derive the elevation of the glacial lakes.
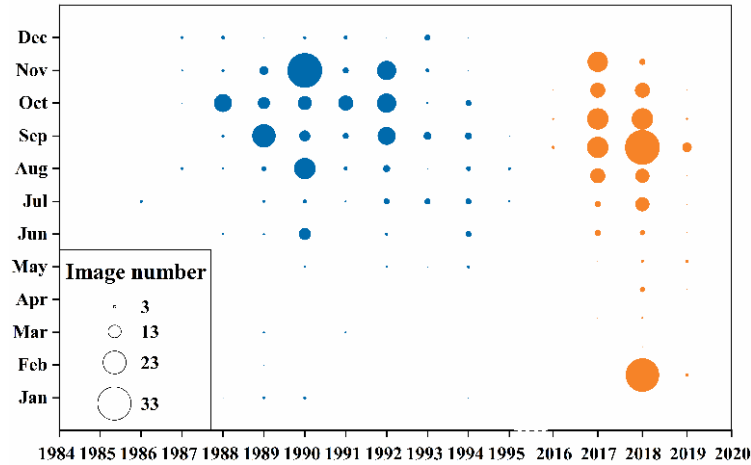
3 Figure 2. Time phases of remote sensing images selected for High Mountain Asia glacial lake inventory.

5 4 Glacial lake inventory methods

6 4.1 Outline of workflow

7   The methods and workflow adopted in this study to produce the glacial lake inventory mainly

8 included collation of knowledge and formulation of the specifications of the glacial lake inventory, data

9 pre-processing, manual vectorization of glacial lakes, interactive checking and error controlling, and

10 attribute database assignment (Fig. 3).

11   (1) Collation of available knowledge regarding glacial lake inventories. As much literature as

12 possible relevant to the investigation and recording of glacial lakes was collected. The various

13 definitions and classifications of glacial lakes, as well as the methods adopted previously for glacial

14 lake boundary extraction and assessment of the extent of glacial lake distributions, were summarized

15 and normative rules formulated for the HMA glacial lake inventory, as explained further in Sect. 4.2.

16   (2) Formulation of the specifications of lake identification. First, a working group of four leading

17 experts in the field was founded in 2014 to discuss and formulate the specifications of the glacial lake

18 inventory. Current knowledge regarding identification of lakes from Landsat imagery (e.g., pixel colour,

19 lake shape, and lake background features) and specifications of vectorization (e.g., viewing scale of

20 1:10,000 on a computer screen vectorization of mixed pixels) was discussed and unified operating

1   criteria were compiled to guide the glacial lake inventory operatives. Novice vectorization operatives

2   were trained until their vectorization results met the pre-specifications of the inventory.

3   (3) Pre-processing of remote sensing data. Pre-processing of the Landsat imagery included false

4   colour compositing and calculation of NDWI maps. The false colour composite images were based on

5   combinations of the operating bands of 7, 5, and 2 or 4, 3, and 2 for Landsat TM/ETM+ images and 5,

6   4, and 3 for Landsat OLI images. The preliminary lake extent was extracted automatically from each

7   image over the entire HMA area using the NDWI based on the near infrared band (NIR) and green

8   band (GREEN), which represent the minimum and maximum water reflectance, respectively

9   (McFeeters, 1996; Zhai et al., 2015; Li et al., 2016; Zhang et al., 2018):

10   $$\mathrm{NDWI} = \frac{B_{GREEN} - B_{NIR}}{B_{GREEN} + B_{NIR}} \qquad (1)$$

11   where B_i is the spectral band of Landsat imagery. The NDWI maps were calculated for each selected

12   Landsat image using different region-specific thresholds. Liu et al. (2016) and Du et al. (2014)

13   suggested that it might be preferable to set the optimized threshold of NDWI$_{GREEN/NIR}$ of Landsat OLI

14   images to −0.05. By considering the edge effects according to the mixed pixels, this study initially

15   selected a lower optimal threshold (approx. −0.1) for specific images to obtain the maximum water

16   body. Then, higher thresholds were tested for visual water extraction before a suitable threshold (varied

17   in the range of −0.10 to 0.20) was selected for a given image to obtain the NDWI map. When manual

18   vectorization was performed on a false colour composite image, the NDWI maps of potential glacial

19   lakes were overlaid to assist in glacial lake identification.

20   (4) Manual vectorization and entering of attribute data. The inventory work was performed during

21   2014–2019. Seven groups were formed to conduct lake boundary vectorization of the 13 HMA

22   sub-regions. After vectorization of a glacial lake, it was required that manual attribute items (e.g., data

23   source and lake type) be input concurrently.

24   (5) Interactive checking and accuracy control. First, glacial lakes were discerned via human–

25   computer interaction, i.e., potential glacial lakes were revealed by the NDWI maps or identified

26   visually from the false colour composite images. Second, glacial lake boundary vectorization results

27   were checked interactively by another vectorization operative to eliminate misclassified areas of

28   shadow and ice and to add areas of glacial lakes evidently omitted in the boundary extraction process.

29   This checking process also minimized the subjective judgment errors of the operatives. Third, attribute

30   items such as glacial lake classification, new/disappeared lakes, and separated/coalesced lakes were

1 checked interactively. In this process, Google Earth imagery was used as an important auxiliary

2 reference data source for error examination.
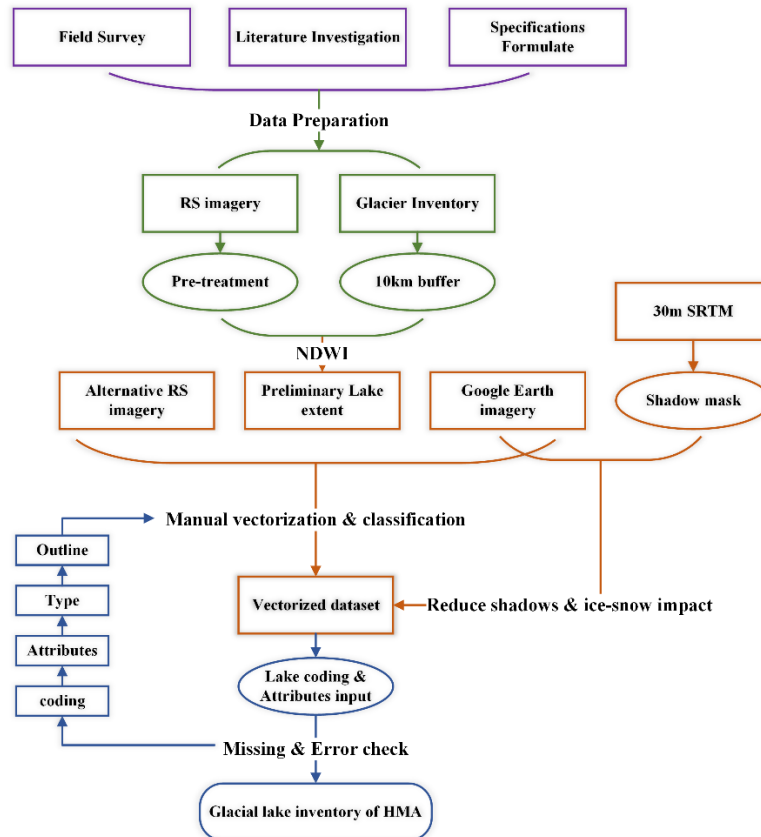
4 Figure 3. Flow chart of HMA glacial lake inventory.

5 **4.2 Illustration of key methods**

6 **4.2.1 Definition of glacial lakes**

7 The definition of a glacial lake determines the type of cryosphere water body that will be recorded

8 as a glacial lake. There are multiple definitions of a glacial lake based on different perspectives (Mool

9 et al., 2001; Yao et al., 2018). When glacial lake inventories are undertaken, most emphasize the

10 elementary role of glaciation in the formation of glacial lakes (Clague and Evans, 2000; Mool et al.,

11 2001). The remarkable difference is whether the period of glaciation or the supply source of glacial

lakes is given greatest attention. Some studies that focused on the former proposed that a glacial lake is a natural water body formed by alpine glacier movement since the Last Glacial Maximum, i.e., ancient or modern glaciers (Liu et al., 1988; Costa and Schuster, 1988). However, other studies emphasized the relation of glacial lakes to meltwater in glaciated areas (Wang et al., 2013; Wang et al., 2014; Zhang et al., 2015). The glacial lake inventory data compiled in this study are intended for use both in water source evaluation and in assessment of environmental change in the alpine cryosphere. Thus, lakes related to glaciers or to glaciation in the alpine cryosphere were all recorded as glacial lakes.

Most Quaternary glaciers have disappeared and the remaining relics are incomplete, which makes it difficult to recover a continuous and complete glaciation range in alpine regions. Thus, it is of great importance to ensure the range of glaciation in an alpine region when conducting a glacial lake inventory based on remote sensing data. The most practical approach might be to specify an indicator threshold to define the glaciation extent according to relevant findings of existing glacier relics in a typical region. On the one hand, the glaciation frontier can usually be indicated by a specified lowest elevation threshold, which is generally closely related to the regional climatic context caused by the elevation effect. However, the lowest elevation threshold might vary enormously with respect to different regions because regional climatic settings differ. For instance, the lowest elevations of 1700 m in Austria (Buckel et al., 2018), 2000 m in Pakistan (Senese et al., 2018), 3000 m in Nepal and Bhutan (Mool et al., 2001), and 3500 m in Peru (Hanshaw and Bookhagen, 2014) were used as specified elevation thresholds to record glacial lakes. On the other hand, defining glaciation extent within a specific distance from modern glacier terminals could be more suitable for the establishment of a glacial lake inventory in relatively large-scale regions with complex regional climate, because the differing climate within large-scale regions can be indicated approximately by the lowest elevation of individual glacier terminals. Some studies adopted distances of 2, 3, or 10 km from modern glacier terminals as thresholds with which to define areas of glacial lakes (Petrov et al., 2017; Veh et al., 2018; Wang et al., 2012, 2013). Distances of 2, 5, 10, and 20 km were considered by Zhang et al. (2015). They found that a distance of 10 km from a modern glacier terminal might be a reasonable guide to glaciation extent and a threshold suitable for a glacial lake inventory of the Tibetan Plateau. This was supported by the finding that the most distant glacierized boundary of the Little Ice Age was up to 10 km from the modern glaciers in the Himalaya area (Wang et al., 2012; Nie et al., 2017). Additionally, to record glacial lakes more precisely, combined distance and elevation thresholds have been used simultaneously to define areas of glacial lakes in special small regions, e.g., lakes at elevations above 1500 m and within

1 2 km of modern glaciers were recorded as glacial lakes in Uzbekistan (Petrov et al., 2017). In this study,

2 given the large scale of the HMA region with its complex climatic context and extremely varied terrain,

3 the data set compiled included glacial lakes within a buffer zone of 10 km from modern glacier extent,

4 which covered an area of approximately $1.25 \times 10^6\,km^2$ according to the Second Glacier Inventory of

5 China and RGI 6.0 (Fig. 1).

6 **4.2.2 Classification of glacial lakes**

7 In glaciation regions, the characteristics of glacial lakes, which include the phase of lake formation,

8 lake basin topography, dam material constituents, geometrical relationship with modern glaciers, and

9 source of water supply (or combinations thereof), have been employed as the basis for glacial lake

10 classification systems (Huggel et al., 2002; Liu et al., 1988; Mool et al., 2001; Yao et al., 2018). For

11 instance, based on lake basin topography, lakes in an inventory of the Hindu Kush--Himalaya region

12 were classified as erosion lakes, valley trough lakes, cirque lakes, blocked lakes, lateral and end

13 moraine-dammed lakes, and supraglacial lakes (Liu et al., 1988; Mool et al., 2001). Recently, Yao et al.

14 (2018) presented a complete classification schema for glacial lake inventory and study of glacial lake

15 hazards that included six classes and eight sub-classes based mainly on the mechanism of glacial lake

16 formation, lake basin topography, and the geometrical relationship with modern glaciers.

17 Generally, it is a little difficult to distinguish glacial lake type in terms of material properties,

18 topographic features, and phase of lake formation using remote sensing imagery. Moreover, most of the

19 standards mentioned above were found inapplicable in previous studies of glacial lake classification in

20 large-scale regions such as HMA because of the lack of enough remote sensing data with satisfactory

21 spatial resolution. In this study, the hydrologic relationship between glacial lakes and modern glaciers

22 was adopted as a classification criterion because the present data set is intended to provide fundamental

23 data for water resource evaluation and glacier hazard assessment. Consequently, glacial lakes were

24 divided into just two types: glacier-fed lakes and non-glacier-fed lakes. The glacier-fed lakes were

25 further divided into three sub-classes: supraglacial lakes (lakes developed on glacier surface),

26 ice-contacted lakes (lakes contacting the glacier terminal or margin), and ice-uncontacted lakes (lakes

27 not contacting the glacier but fed directly by glacial meltwater). This classification was based on

28 whether the surface hydrological flow of the modern glacier and topographic features of the lake basin

29 allowed a lake to receive meltwater from the modern glacier. To achieve reliable classification results,

30 glacial lakes were distinguished with the assistance of 3D digital terrain imagery from Google Earth, a

Shuttle Radar Topography Mission digital elevation model, and glacier outlines from RGI 6.0. Based on visual inspection of the satellite images and with reference to 3D digital terrain imagery from Google Earth, we recorded a glacier-fed lake when (1) a lake had lower elevation than the modern glacier (mother glacier) and (2) the mother glacier(s) meltwater could flow into the lake via surface channel. It is common for glacial lakes to be fed by meltwater through subsurface channels; however, we ignored this because it is difficult to survey the subsurface channels of glacial lakes using remote sensing data. In addition, lake type was distinguished based on the topographic features of the lake basin and the modern glaciers; in most cases, it is possible that the lakes were fed by meltwater flowing through both sub-surface and surface channels.

4.2.3 Extraction of lake boundary

This study adopted automatic glacial lake extraction and manual glacial lake boundary vectorization to determine glacial lake boundaries. In the NDWI-based automatic lake boundary extraction approach, two bands were selected to facilitate a ratio calculation to maximize the difference between water and non-water objects in the remote sensing imagery based on a given threshold. The given threshold was determined subjectively with consideration of how much detailed information of the lake water bodies was captured precisely. The given threshold was varied to account for various factors such as the differences in Landsat sensors (i.e., TM, ETM+, and OLI), time phase of images, quality of images, and complexity of surface features. To achieve the optimal threshold for lake water body recognition, the candidate threshold was debugged iteratively for each image. In practice, because the area of the glacial lakes was usually small (see next paragraph) and the spectral features of the lake water bodies were varied, the threshold had to be set to allow capture of the greatest number of water body pixels, which consequently resulted in simultaneous acquisition of more non-lake-water-body noise information. It also resulted in more effort in the subsequent manual modification to reduce noise information using methods such as algorithms to eliminate mountain shadows (Gardelle et al., 2011).

Manual visual vectorization distinguishes lake boundaries by identifying the unique texture, colour, and other characteristics of glacial lakes in false colour composite images based on available professional knowledge and accumulated experience in vectorization operations. Even though it was regarded a time-consuming and labour-intensive process, it was also considered an attractive approach because of its consistency, high level of quality control, and reasonably simple operational procedure, given the varied quality of Landsat images available for the large-scale HMA region. In this study, the

1 manual visual vectorization process was generally found more suitable in terms of effort and precision

2 for generating a glacial lake inventory data set of the HMA region in comparison with automatic glacial

3 lake extraction. Therefore, manual visual vectorization in conjunction with NDWI maps was the main

4 method adopted to extract glacial lake boundaries to minimize the deficiencies produced by individual

5 subjectivity of the operatives.

6   The minimum number of pixels used to extract a glacial lake water body was found inconsistent in

7 the available literature. For example, arbitrary threshold areas of 0.0027 km^2 (three lake water body

8 pixels) (Zhang et al., 2015) and 0.0081 km^2 (nine lake water body pixels) (Nie et al., 2017) have been

9 used in earlier glacial lake investigations. Moreover, minimum threshold areas of 0.01 km^2

10 (approximately 10 lake water body pixels), 0.02 km^2 (approximately 22 lake water body pixels), and

11 0.1 km^2 (approximately 111 lake water body pixels) have also been set to evaluate the level of risk of

12 glacial lake outburst floods in the Himalaya and Tien Shan Mountains (Petrov et al., 2017; Wang et al.,

13 2013; Worni et al., 2013; Bolch et al., 2011; Allen et al., 2019). Theoretically, one pure pixel of a lake

14 water body could be recorded as a glacial lake. However, a glacial lake is generally not represented by

15 one pure pixel unless it is aligned perfectly with the raster grid; usually, it would be surrounded partly

16 or fully by 1–8 mixed lake water body pixels (Fig. 4a, b). Consequently, manual delineation was

17 required for approximately 1/2, 1/8, or 7/8 of the peripheral mixed pixels surrounding pure lake water

18 body pixels (Fig. 4-d, e). If 3 or 4 pure lake water body pixels exist in a Landsat image, the maximum

19 number of peripheral mixed pixels is 12 (Fig. 4d, e). Usually, for three pure lake water body pixels, the

20 ratio of the area of pure lake water body pixels to the area of peripheral mixed pixels can be expressed

21 as follows:

22    $$\frac{\text{Area of peripheral mixed pixels}}{\text{Area of three pure lake water body pixels}} \times 100\% = \frac{6\times\frac{1}{2}+5\times\frac{1}{8}+1\times\frac{7}{8}}{3} \times 100\% = 150\%. \qquad (2)$$

23 For four pure lake water body pixels, the ratio of the area of pure lake water body pixels to the area of

24 peripheral mixed pixels is:

25    $$\frac{\text{Area of peripheral mixed pixels}}{\text{Area of four pure lake water body pixels}} \times 100\% = \frac{8\times\frac{1}{2}+4\times\frac{1}{8}}{4} \times 100\% = 112.5\%. \qquad (3)$$

26 Thus, in this study, the minimum glacial lake area recorded was set at 0.0054 km2 (e.g., 3–4 pure lake

27 water body pixels with approximately 12 peripheral mixed pixels, which equate to approximately 6 full

28 lake water body pixels) because a lake area covering fewer than three pure lake water pixels could

29 possibly have an error of >100 % (Fig. 4b, c) despite the revised coefficient of one standard deviation

30 (0.6872) involved (see Sect. 5).
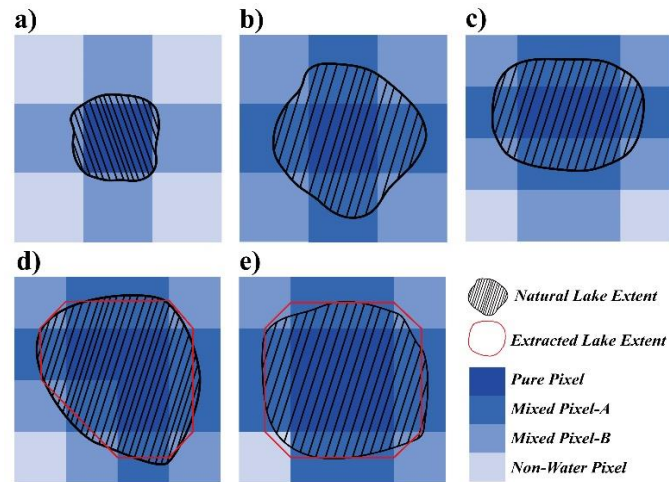
3   Figure 4. Sketches showing the relationships of pure water body pixels and surrounding potential

4   mixed water body pixels: (a) a pure water body pixel surrounded by four potential mixed water body

5   pixels, (b) a pure water body pixel surrounded by eight potential mixed water body pixels, (c) 2 pure

6   water body pixels surrounded by 10 potential mixed water body pixels, (d) 3 pure water body pixels

7   with 12 surrounding potential mixed water body pixels, and (e) 4 pure water body pixels with 12

8   surrounding potential mixed water body pixels.

9   **4.2.4 Input of attribute items**

10   Eight attribute items were input into the HMA glacial lake inventory: lake coding, location

11   (longitude, latitude, and elevation), perimeter, area, type, area error, time phase, source image

12   information, and sub-region of located lake. (1) We encoded each glacial lake based on its central

13   location using the same coding format as used by the National Snow and Ice Data Centre to encode

14   glaciers. The code can be expressed as "GLmmmmmmEnnnnnN", where m and n represent the results

15   of the longitude and latitude of each glacial lake centroid multiplied by 1000, respectively, GL is the

16   abbreviation of glacial lake, and E and N represent eastings and northings, respectively. (2) The

17   location information of each glacial lake was labelled as the geographic coordinates of the centroid of

18   the shape of each glacial lake, calculated using ArcMap software. The lake elevation was defined as the

19   average elevation of a buffer zone of 30 m radius centred on the glacial lake centroid, which was

20   derived from the Shuttle Radar Topography Mission digital elevation model. (3) The area and

perimeter of each lake were calculated using ArcMap based on the unified geography coordinate system of GCS_WGS_1984 and the Asia_North_Albers_Equal_Area_Conic projection system, respectively, to avoid errors caused by projection deformation. (4) The error of lake area was calculated using Eqs. (4) and (5) (Sect. 5). (5) Lake type, which was input manually, was defined as either supraglacial lake, ice-contacted lake, ice-uncontacted lake, or non-glacier-fed lake (see Sect. 4.2.2). (6) Lake time phase was the acquisition date of the original Landsat image, which was recorded as the time phase for each lake. (7) Source image information referred to the image number of the Landsat images used to extract the glacial lake boundary. (8) The sub-region to which each lake belonged identified the regional location within the HMA area. Each lake was assigned based on shp. file data of the boundaries of the 13 HMA sub-regions, obtained from the National Snow and Ice Data Centre, using the ArcMap spatial analysis tool.

5 Error assessment

The errors associated with glacial lake extraction from remote sensing imagery using manual visual delineation are generally related to components of the quality of the images (e.g., spatiotemporal resolution, cloud coverage, and mountain shadows), experience, operative subjectivity, and the threshold area of the inventory (Gardelle et al., 2011; Hall et al., 2003; Paul et al., 2004; Salerno et al., 2012; Zhang et al., 2015). It has been reported that the area error of glacial lake boundary extraction based on remote sensing images can be approximately ±0.5 pixels depending on the quality of the imagery (Fujita et al., 2009; Salerno et al., 2012). Furthermore, the area error of glacial lake delineation attributable to manual delineation can be assumed to follow a Gaussian distribution (Hanshaw and Bookhagen, 2014). Hence, the theoretical maximum area error of glacial lake boundary extraction is the half-area of the edge pixels because pure lake water body pixels are usually surrounded by mixed pixels (Fig. 4). The lake area error of a single glacial lake within one standard deviation (1σ) can be expressed as follows (Hanshaw and Bookhagen, 2014):

$$\text{Error}(1\sigma) = \frac{P}{G} \times \frac{G^2}{2} \times 0.6872, \tag{4}$$

$$E = \frac{\text{Error}(1\sigma)}{A} \times 100\ \%, \tag{5}$$

where P is the perimeter of the glacial lake (m), G is the spatial resolution of the remote sensing imagery (30 m in this data set), 0.6872 is the revised coefficient under 1σ (i.e., approximately 69 % of peripheral pixels are subjected to errors), E is the relative error of the glacial lake, and A is the total

area of the glacial lake. Then the accumulation of errors of all the lake areas for the entire study region or subregions can be calculated using the following formula based on error propagation theory:

$$E_T = \sqrt{\sum_{i=1}^{n} a_i^2} \, , \tag{6}$$

where E_T is the area error of the entire study region or subregions, i is the lake of No. i in the entire study region or sub-regions, and a is the error area of a single lake.

The resulting calculated error indicated that the total absolute area error of HMA glacial lakes was approximately ± 2.11 and ± 2.28 km^2 and the average relative error was ± 13.5 and ± 13.2 % in 1990 and 2018, respectively. The relative area errors of each lake varied from 1–79 %, and a significant power exponential relationship was found between the relative area error and the sizes of the glacial lakes ($E = 0.050A^{-0.45}$, $R^2 = 0.96$, $\alpha < 0.001$) (Fig. 5a). Small-sized lakes (i.e., area ≤ 0.01 km^2, which accounted for 2 % of the total lake area in HMA) had the largest average relative area error of 44.6 % (Fig. 5b). Medium-sized lakes (i.e., area of 0.01–0.1 km^2, which accounted for 34 % of the total lake area in HMA) had an average relative area error of 22.0 % (Fig. 5c). Large-sized lakes (i.e., area ≥ 0.1 km^2, which accounted for 64 % of the total lake area in HMA) had the smallest average relative area error of 7.6 % (Fig. 5d). In summary, smaller glacial lakes in the HMA region had larger relative area errors, and vice versa.

To further verify the accuracy of the manual delineation of glacial lake boundaries, nine lakes located within the HMA region were surveyed using a portable GPS device (Trimble GeoXH6000) with decimetre accuracy during July–August 2018 (Fig. 6). The lakes selected for field survey covered areas of 0.01–2.97 km^2. The field-based lake boundaries were compared with those obtained via manual delineation (i.e., derived from Landsat OLI imagery acquired during 2018). It was found that the area error (i.e., the percentage difference of the absolute area encircled by the manually delineated lake boundary and that derived by the GPS survey) varied from 5.5–25.5 %. Moreover, it was determined that the average horizontal distance deviation between the two types of boundary varied from 4.5–33.5 m (Table 1). Overall, the horizontal deviations were largely confined to one pixel, and the average accuracy of the delineation of glacial lake boundaries was within ± 0.5 pixels (± 15 m).
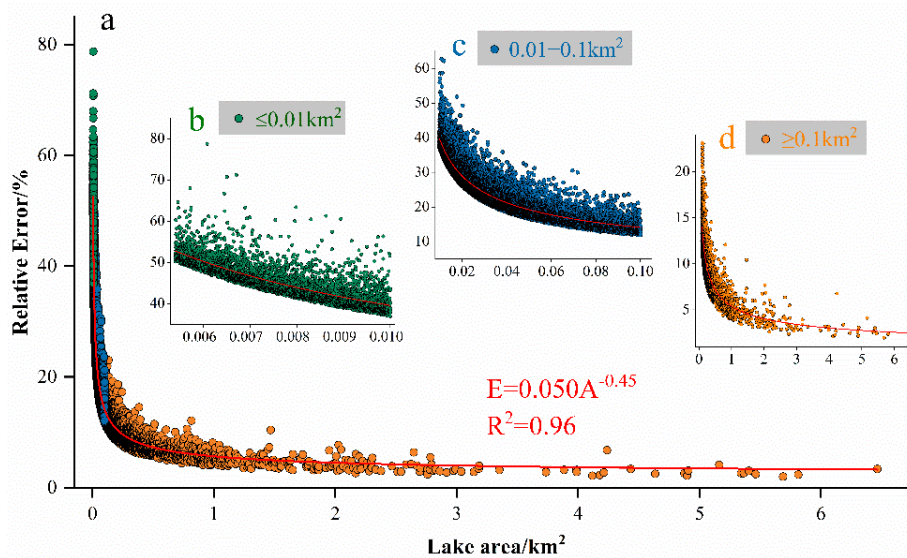
2 Figure 5. Relationships of relative area error against size of glacial lakes in HMA: (a) relationship for

3   glacial lakes of all sizes and (b)–(d) relationships for glacial lakes of specific size.

5 Table 1. Horizontal deviations between lake boundaries obtained by manual delineation and field

6   survey using a portable GPS device (Trimble GeoXH6000)

Name (labelled in Figure 6)	Lake ID	Lake size (km²)	Horizontal deviations of delineation boundary (m)			Area error(%)
			minimum	maximum	average	
Qiongyong Cuo (A)	GL090225E28890N	0.08	-7.6	9.1	4.5	5.5
Passu Lake (B)	GL074878E36457N	0.15	-10.9	12.0	6.0	6.8
Longbasa Lake (C)	GL088071E27950N	1.49	-22.7	-8.4	12.4	/
Zongge Cuo (D)	GL087654E28113N	1.48	-26.8	24.9	13.5	6.1
Unnamed (E)	GL088151E28010N	0.01	-4.7	4.8	3.2	16.3
Unnamed (F)	GL088257E28011N	0.58	-12.9	12.4	4.6	/
Unnamed (G)	GL088240E28005N	0.40	-20.8	15.9	7.1	/
Large Laigu Lake (H)	GL096818E29298N	2.97	-36.7	-6.4	15.3	/
Small laigu Lake (I)	GL096832E29294N	1.02	-32.8	17.6	9.8	/

7 Note: "/" indicates the sample lake boundary was only partly surveyed using the handheld GPS device.
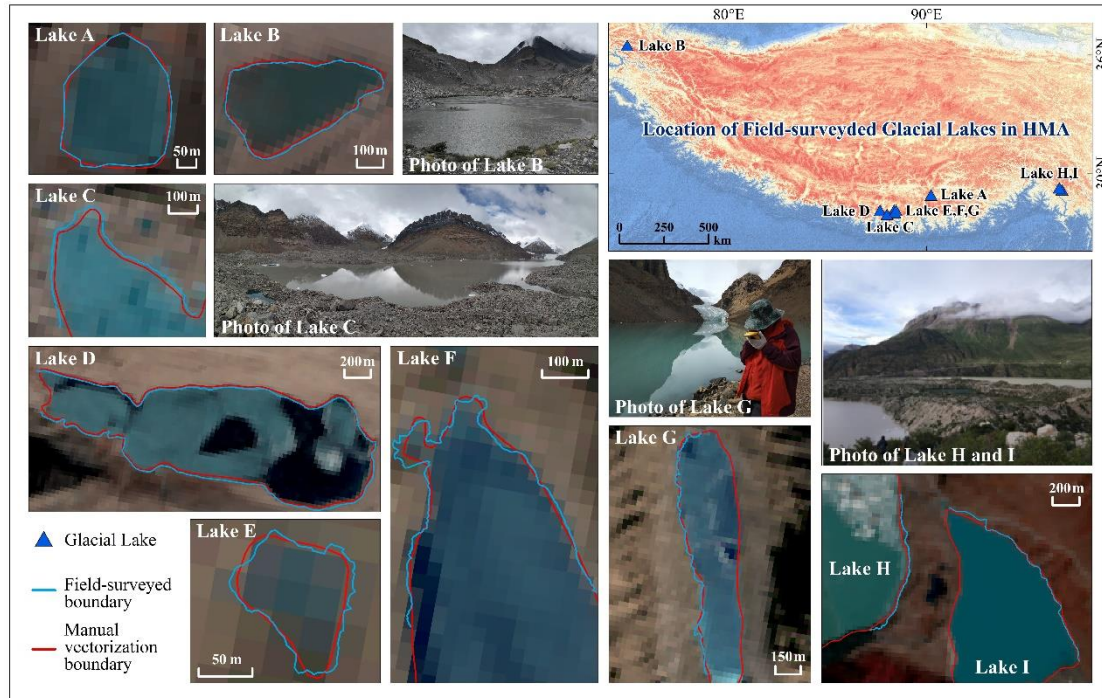
3 Figure 6. Glacial lakes in the HMA region surveyed in summer 2018 (the backgrounds of the surveyed

4 lakes are Landsat OLI images).

5 **6 Distribution and changes of HMA glacial lakes**

6   As indicated by the achieved HMA glacial lake inventory, 30,121 (2080.12 $\pm$ 2.28 km^2) glacial

7 lakes were identified in 2018 and their distribution had considerable spatial heterogeneity (Fig. 7). The

8 greatest concentration of glacial lakes was in Altay and Sayan (335.42 $\pm$ 0.88 km^2, which accounted for

9 16.1 % of the total area of glacial lakes) and Eastern Himalaya (310.37 $\pm$ 0.89 km^2, which accounted for

10 14.9 % of the total area of glacial lakes). Relatively few glacial lakes were found distributed in Eastern

11 Kun Lun and Qilian Shan (38.85 $\pm$ 0.29 km^2, which accounted for 1.9 % of the total area of glacial lakes)

12 and Eastern Tien Shan (40.55 $\pm$ 0.32 km^2, which accounted for 2.0 % of the total area of glacial lakes).

13 The HMA glacial lakes were located within the elevation range of 1357–6247 m in 2018. An

14 approximate normal distribution was presented both for the lakes of the entire HMA region and for the

15 lakes in most sub-regions. More than 43 % of the HMA lake area has survived within the vertical range of

16 4500–5400 m, with the peak lake area of 241.89 $\pm$ 0.80 km^2 (accounting for 11.6 % of the total area) in

1 the range of 5100–5300 m. The elevation band of peak lake area in the different sub-regions varied from

2 2300–2500 m in Altay and Sayan to 5300–5500 m in Central Himalaya, Karakoram, and Western Kun

3 Lun.
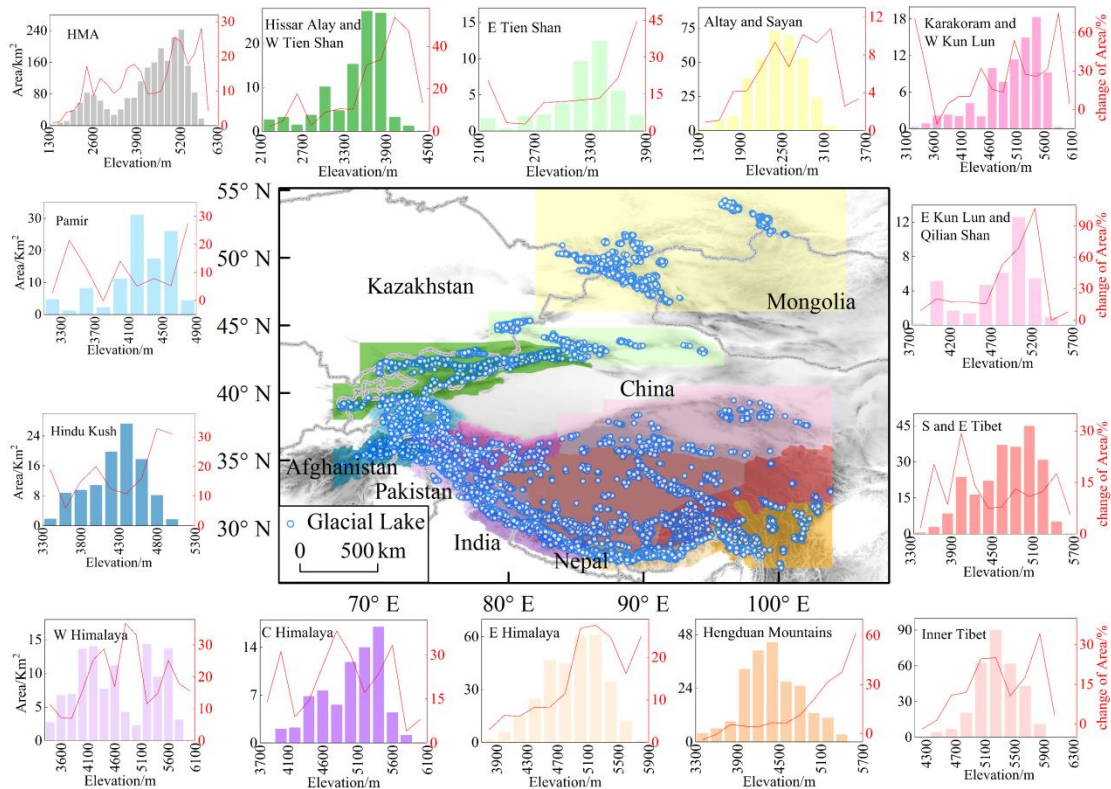
6 Figure 7. Distribution and change of glacial lake area in the entire HMA and its 13 sub-regions from

7 1990–2018.

9   The HMA glacial lakes experienced widespread areal expansion during 1990–2018 with an

10 average rate of increase in area of 15.2 % (Fig. 7). The rate of change of area varied widely between

11 different sub-regions and different 200 m elevation bands. The glacial lakes in Eastern Kun Lun and

12 Qilian Shan experienced the most rapid expansion in area during 1990–2018 with an average rate of

13 increase of 45.6 %, whereas the rate of change was only 7.5 % in Altay and Sayan. Glacial lakes have

14 tended to develop to higher elevations during recent decades with the maximum distribution elevation

1   of 6078 m in 1990 rising to 6247 m in 2018. The rate of change of glacial lakes in the different 200 m

2   elevation bands presented a large average trend against elevation, rising as a whole during 1990–2018

3   (Fig. 7). The lake area expanded most from the elevation of approximately 5000 m and the rate of

4   expansion reached approximately 28 % at 5700–5900 m in the entire HMA region, although it differed

5   between different sub-regions. Lake area showed a notable rate of increase with elevation in most

6   sub-regions, e.g., Hissar Alay and Western Tien Shan, Hindu Kush, Eastern Himalaya, Hengduan

7   Mountains, Eastern Tien Shan, and Altay and Sayan. The rate of expansion varied markedly and no

8   observable trends in the rate of increase or decrease with elevation were discovered in Karakoram and

9   Western Kun Lun, Western Himalaya, and Inner Tibet. The rate of expansion in Central Himalaya and

10 Southern and Eastern Tibet was found to have seemingly decreased with increasing elevation (Fig. 7).

11 **7 Comparison and limitations**

12   There are at least 34 published reports or data sets on the regional extent of glacial lakes in the

13 HMA area, which are based on various lake boundary extraction methods and different data sources

14 (Supplementary Table S1). This previous research work examined glacial lakes from as early as 1962

15 up until 2017. However, it is difficult to evaluate any discrepancies comprehensively because different

16 extents of glacial lake distribution were examined and inconsistent thresholds of minimum lake area

17 were used. Glacial lake inventory data of the Third Pole region in 1990 (Zhang et al., 2015) and of the

18 HMA (Chen et al., 2020) in 2017 were used for comparison because both recorded glacial lakes in the

19 same buffer zone (i.e., within 10 km of the modern glacier extent) and over similar periods. For the

20 comparison, the same thresholds and regions were adopted for the inventory data. Marked

21 discrepancies were found to exist between the different datasets in terms of both the number and the

22 area of the glacial lakes. In 1990, only 4601 glacial lakes ($\geq$0.0054 km^2) with total area of 554.33 km^2

23 were recorded by Zhang et al. (2015), whereas 20,410 glacial lakes with total area of 1376.23 km^2 were

24 catalogued in the Third Pole region in this study. In 2017, 14,477 glacial lakes with total area of

25 1635.94 km^2 were recorded by Chen et al. (2020), whereas, we recorded 22,727 glacial lakes ($\geq$0.0081

26 km^2) with total area of 1726.41 km^2 in 2018 in HMA (excluding Altay and Sayan). We consider the

27 discrepancies attributable to three primary factors. (1) The buffer zone within 10 km of the modern

28 glacier extent was inconsistent between the data sets because different glacier inventories were used. (2)

29 Different operatives catalogued the glacial lakes using different remote sensing data covering different

30 periods. (3) Many glacial lakes were possibly missed because of the comparatively less manual

1 vectorization effort involved in the work of Zhang et al. (2015) and Chen et al. (2020). Overall, our

2 glacial lake inventory catalogued glacial lakes throughout the entire HMA more comprehensively and

3 with more careful error assessment when compared with available glacial lake data sets from regional

4 or river-basin-based studies.

5   Several limitations deserve proper consideration when using the glacial lake inventory data. First,

6 a degree of uncertainty resulted from using Landsat image data that covered different periods, i.e., both

7 interannually and seasonally. Although images acquired in summer or autumn (June–November) were

8 set as optimal choices, the selected images covered most seasons of the year, e.g., the images selected

9 in June–November accounted for only 72.3 and 88.8 % of the total number in 2018 and 1990,

10 respectively. Interannually,   images were selected from a span of 10 years (1986–1995) and 4 years

11 (2016–2019) to obtain sufficient high-quality images of the HMA area. Second, this study recorded all

12 lakes located within the 10 km buffer area of glacier extent as glacial lakes. Therefore, certain lakes

13 that have no relation to glaciers or to glaciation (i.e., non-glacial lakes) in the alpine cryosphere were

14 potentially catalogued in error because of the difficulty in distinguishing non-glacial lakes from glacial

15 lakes based on remote sensing data. Third, we identified water bodies related to glaciers or to glaciation

16 in the alpine cryosphere as glacial lakes. However, in many cases, it was difficult to determine whether

17 such bodies should be recorded as glacial lakes, e.g., cases of long narrow water bodies on rivers and

18 cases where the number of pure water body pixels was small. Thus, some errors and inconsistences

19 were inevitable because of having different operatives performing the lake boundary vectorization and

20 inspection. In future, this glacial lake inventory will be updated and shared on the National Special

21 Environment and Function of Observation and Research Stations Shared Service Platform (China).

22 **8 Data availability**

23   The data set developed in this study comprises two .shp file documents containing the glacial lake

24 inventory of the HMA region in 1990 and 2018. The data set can now be accessed via the website of

25 the National Special Environment and Function of Observation and Research Stations Shared Service

26 Platform (China): http://www.crensed.ac.cn/portal/metadata/706ce17f-1684-4e8d-bf5e-7d517e03693c

27 (Wang et al., 2019a).

28 **9 Conclusions**

29   A glacial lake inventory of the HMA region was realized based on satellite remote sensing data

30 and GIS techniques. Eight attribute items were recorded in the glacial lake inventory data set of the

HMA region. Lake area error was assessed carefully with respect to theoretical analysis of lake boundary pixels and actual boundaries derived by GPS field-based surveys. On average, the deviations between the delineation of lake boundaries derived using the two methods were within ±0.5 pixels (±15 m). The relative area errors of each lake in 2018 varied from 1–79 %, and the average relative area errors of ±13.2 % in the entire HMA region were characterized by increase in the relative area error with decreasing lake size.

Overall, 30,121 glacial lakes with a total area of 2080.12 ± 2.28 km^2 were catalogued in 2018 in the HMA region. Glacial lakes survived in all 13 sub-regions of HMA from the elevation of 1357 to 6247 m. Glacial lakes were found concentrated in the sub-regions of Altay and Sayan and Eastern Himalaya and at elevation bands of 4500–5400 m. The HMA glacial lakes have experienced widespread expansion with an average rate of increase in area of 15.2 %. Lake area expanded most in the higher elevation bands during 1990–2018. The data set is expected to provide basic data to support cryosphere hydrology research, water resources utilization and management, and assessment of glacier-related hazards in the HMA region.

10 Acknowledgements

The study was funded by the National Natural Science Foundation of China (No. 41771075, No. 41571061, and No. 41271091). The authors are grateful to the lake boundary vectorization operators who were not included as authors: Yao Chao, Chen Shiyin, Zhu Xiaoxi, Li Ruijia, Huang Rong, Peng Xin, Xiang Lili, Yi Ying, Liu Yanlin, Fu Yongqiao, Ran Weijie, and Gu Ju. We thank James Buxton MSc from Liwen Bianji, Edanz Group China (https://en-author-services.edanzgroup.com/), for editing the English text of this manuscript.

11 References

Allen, S. K., Zhang, G., Wang, W., Yao, T., and Bolch, T.: Potentially dangerous glacial lakes across the Tibetan Plateau revealed using a large-scale automated assessment approach, Sci. Bull., 64, 435-445, doi.org/10.1016/j.scib.2019.03.011, 2019.

Arendt, A., Bliss, A., Bolch, T., Pfeffer, W. T., Cogley, J. G., and Gardner, A. S.: Randolph Glacier Inventory – A Dataset of Global Glacier Outlines: Version 5.0, Boulder Colorado, USA, 2015.

Bolch, T., Kulkarni, A., Kääb, A., Huggel, C., Paul, F., Cogley, J. G., Frey, H., Kargel, J. S., Fujita, K., Scheel, M., Bajracharya, S., and Stoffel, M.: The State and Fate of Himalayan Glaciers, Science, 336, 310–314 , doi:10.1126/science.1215828 , 2012.

Bolch, T., Peters, J., Yegorov, A., Pradhan, B., Buchroithner, M., and Blagoveshchensky, V.: Identification of potentially dangerous glacial lakes in the northern Tien Shan, Nat. Hazards, 59, 1691-1714, doi:10.1007/s11069-011-9860-2, 2011.

Brun, F., Berthier, E., Wagnon, P., Kääb, A., and Treichler, D.: A spatially resolved estimate of High Mountain Asia glacier mass balances,2000-2016, Nat. Geosci, 10, 668-673, doi:10.1038/NGEO2999, 2017.

Buckel, J., Otto, J. C., Prasicek, G., and Keuschnig, M.: Glacial lakes in Austria - Distribution and formation since the Little Ice Age, Global, 164, 39-51, doi:10.1016/j.gloplacha.2018.03.003, 2018.

Chen, F., Zhang, M., Guo, H., Allen, S., Kargel, J. S., Haritashya, U. K., and Watson, C. S.: Annual 30-meter Dataset for Glacial Lakes in High Mountain Asia from 2008 to 2017, Earth Syst. Sci. Data Discuss., 1-29, https://doi.org/10.5194/essd-2020-57, 2020. ~~Yang, C., Wang, X., Wei, J., Liu, Q., Lu, A., Zhang, Y., Tang, Z.: Chinese glacial lake inventory based on 3S technology method, J Geogr Sci, 74, 544-556, doi:10.11821/dlxb201903011, 2019.~~

Clague, J. J., and Evans, S. G.: A review of catastrophic drainage of moraine-dammed lakes in British Columbia, Quat. Sci. Rev., 19, 1763-1783, doi:10.1016/s0277-3791(00)00090-1, 2000.

Cook, K. L., Andermann, C., Gimbert, F., Adhikari, B. R., and Hovius, N.: Glacial lake outburst floods as drivers of fluvial erosion in the Himalaya, Science, 362, 53–57, doi:10.1126/science.aat4981, 2018.

Costa, J. E., and Schuster, R. L.: The formation and failure of natural dams, Geol. Soc. Am. Bull., 100, 1054-1068, doi:10.1130/0016-7606(1988)1002.3.CO;2, 1988.

Du, Z., Li, W., Zhou, D., Tian, L., Ling, F., Wang, H., Gui, Y., and Sun, B.: Analysis of Landsat-8 OLI imagery for land surface water mapping, Remote Sens. Lett., 5, 672-681, doi:10.1080/2150704x.2014.960606, 2014.

Fujita, K., Sakai, A., Nuimura, T., Yamaguchi, S., and Sharma, R. R.: Recent changes in Imja glacial lake and its damming moraine in the Nepal Himalaya revealed by in situ surveys and multi-temporal ASTER imagery, Environ. Res. Lett., 4, 045205, doi:10.1088/1748-9326/4/4/045205, 2009.

Gardelle, J., Yves, A., and Etienne, B.: Contrasted evolution of glacial lakes along the Hindu Kush Himalaya mountain range between 1990 and 2009, Global, 75, 47-55, doi:10.1016/j.gloplacha.2010.10.003, 2011.

Gardner, A. S., Moholdt, G., Graham, C. J., Wouters, J., Arendt, A. A., Wahr, J., Berthier, E., Hock, R., Pfeffer, W. T., Kaser, G., Ligtenberg, S. M. R., Bolch,T. Sharp, M. J., Hagen, J. O., Broeke, M. R. V.

D., and Paul, F.: A Reconciled Estimate of Glacier Contributions to Sea Level Rise: 2003 to 2009, Science, 340, 852–857, doi:10.1126/science.1234532 , 2013.

Haeberli, W., Schaub, Y., Huggel, C.: Increasing risks related to landslides from degrading permafrost into new lakes in de-glaciating mountain ranges, Geomorphology, 293, 405–417, doi: 10.1016/j.geomorph.2016.02.009, 2016.

Hall, D. K., Klaus J. B., Wolfgang S., Bindschadler, R. A., and Chien, J. Y. L.: Consideration of the errors inherent in mapping historical glacier positions in Austria from the ground and space (1893–2001), Remote Sens. Environ, 86, 566-577, doi:10.1016/s0034-4257(03)00134-2, 2003.

Hanshaw, M. N., and Bookhagen, B.: Glacial areas, lake areas, and snow lines from 1975 to 2012: status of the Cordillera Vilcanota, including the Quelccaya Ice Cap, northern central Andes, Peru, The Cryosphere, 8, 359-376, doi:10.5194/tc-8-359-2014, 2014.

Hewitt, K.: The Karakoram Anomaly? Glacier Expansion and the 'Elevation Effect,' Karakoram Himalaya, Mt. Res. Dev., 25, 332-340, doi:10.1659/0276-4741(2005)025 [0332:TKAGEA]2.0.CO;2, 2005.

Hock, R., Rasul G., Adler C., Cáceres B., Gruber S., Hirabayashi Y., Jackson M., Kääb A., Kang S., Kutuzov S., Milner A., Molau U., Morin S., Orlove B., and Steltzer H. High Mountain Areas. In: IPCC Special Report on the Ocean and Cryosphere in a Changing Climate [Pörtner H.-O., Roberts D.C., Masson-Delmotte V., Zhai P., Tignor M., Poloczanska E., Mintenbeck K., Alegría A., Nicolai M., Okem A., Petzold J., Rama B., Weyer N.M. (eds.)], 2019.

Huggel, C., Kääb, A., Haeberli,W., Teysseire, P., and Paul, F.: Remote sensing based assessment of hazards from glacier lake outbursts: a case study in the Swiss Alps, Can. Geotech. J., 39, 316-330, doi:10.1139/t01-099, 2002.

ICMOD: Glacial lakes and glacial lake outburst floods in Nepal, Kathmandu, ICMOD, 2011.

Kääb, A., Berthier, E., Nuth, C., Gardelle, J., and Arnaud, Y.: Contrasting patterns of early twenty-first-century glacier mass change in the Himalayas, Nature, 488, 495-498, doi:10.1038/nature11324, 2012.

Kääb, A., Treichler, D., Nuth, C., and Berthier, E.: Brief Communication: Contending estimates of 2003-2008 glacier mass balance over the Pamir–Karakoram–Himalaya, The Cryosphere, 9, 557–564, doi: 10.5194/tcd-8-5857-2014, 2015.

Li, J., Sheng, Y., and Luo, J.: Automatic extraction of Himalayan glacial lakes with remote sensing, J. Remote Sens., 15, 29-43, doi:10.1631/jzus.C0910717, 2011.

Li, Y., Gong, X., Guo, Z., Xu, K., Hu, D., and Zhou, H.: An index and approach for water extraction using Landsat–OLI data, Int. J. Remote Sens., 37, 3611-3635, doi: 10.1080/01431161.2016.1201228, 2016.

Liu, C., Mayor-Mora, R., Sharma, C. K., Xing, H., and Wu, S.: Report on first expedition to glaciers and glacier lakes in the Pumqu (Arun) and Poiqu (Bhote-SunKosi) River Basin, Xizang (Tibet), China. Beijing: Science Press, 1-192, 1988.

Liu, Z., Yao, Z., and Wang, R.: Assessing methods of identifying open water bodies using Landsat 8 OLI imagery, Environ. Earth Sci., 75, doi:10.1007/s12665-016-5686-2, 2016.

Mcfeeters, S. K.: The use of the Normalized Difference Water Index (NDWI) in the delineation of open water features, Int. J. Remote Sens., 17, 1425-1432, doi: 10.1080/01431169608948714, 1996.

Mool, P. K., Bajracharya, S. R., and Joshi, S. P.: Inventory of glaciers, glacial lakes and glacial lake outburst floods, Nepal. International Centre for Integrated Mountain Development, Kathmandu, Nepal, 2001.

Nie, Y., Sheng, Y., Liu, Q., Liu, L., Liu, S., Zhang, Y., and Song, C.: A regional-scale assessment of Himalayan glacial lake changes using satellite observations from 1990 to 2015, Remote Sens. Environ., 189, 1-13, doi:10.1016/j.rse.2016.11.008, 2017.

Paul, F., Haggel, C., and Kääb,A.: Combining satellite multispectral image data and a digital elevation model for mapping debris-covered glaciers, Remote Sens. Environ, 89, 510-518, doi:10.1016/j.rse.2003.11.007, 2004.

Petrov, M. A., Sabitov, T. Y., Tomashevskaya, I. G., Glazirin, G. E., Chernomorets, S. S., Savernyuk, E. A., Tutubalina, O. V., Petrakov, D. A., Sokolov, L. S., Dokukin, M. D., Mountrakis, G., Ruiz-Villanueva, V., and Stoffel, M.: Glacial lake inventory and lake outburst potential in Uzbekistan, Sci Total Environ, 592, 228-242, doi:10.1016/j.scitotenv.2017.03.068, 2017.

Pfeffer, W., Tad, A. A., Bliss, A., Bolch, T., Cogley, J. G., Gardner, A. S., Hagen, J.-O., Hock, R., Kaser, G., and Kienholz, C.: The Randolph Glacier Inventory: a globally complete inventory of glaciers, J. Glaciol., 60, 537-552, doi:10.3189/2014JoG13J176, 2014.

Salerno, F., Thakuri, S., D'Agata, C., Smiraglia, C., Manfredi, E. C., Viviano, G., and Tartari, G.: Glacial lake distribution in the Mount Everest region: Uncertainty of measurement and conditions of formation, Glob. Planet. Change, 92,30-39, doi:10.1016/j.gloplacha.2012.04.001, 2012.

Senese, A., Maragno, D., Fugazza, D., Soncini, A., D'Agata, C., Azzoni, R. S., Minora, U., Ul-Hassan, R., Vuillermoz, E., Asif Khan, M., Shafiq Rana, A., Rasul, G., Smiraglia, C., and Diolaiuti, G. A.:

Inventory of glaciers and glacial lakes of the Central Karakoram National Park (CKNP-Pakistan), J. Maps ,14, 189-198, doi:10.1080/17445647.2018.1445561, 2018.

Slemmons, K. E., Saros, J. E., and Simon, K.: The influence of glacial meltwater on alpine aquatic ecosystems: a review, Environ Sci Process Impacts, 15, 1794-806, doi: 10.1039/c3em00243h, 2013.

Song, C., Huang, B., Ke, L., and Richards, K. S.: Remote sensing of alpine lake water environment changes on the tibetan plateau and surroundings: A review, Int. J. Remote Sens., 92, 26-37, doi:10.1016/j.isprsjprs.2014.03.001, 2014.

Song, C., Sheng, Y., Ke, L., Nie, Y., and Wang, J.: Glacial lake evolution in the southeastern Tibetan Plateau and the cause of rapid expansion of proglacial lakes linked to glacial-hydrogeomorphic processes, J. Hydrol., 540, 504-514, doi:10.1016/j.jhydrol.2016.06.054, 2016.

Veh, G., Korup, O., Roessner, S., and Walz, A.: Detecting Himalayan glacial lake outburst floods from Landsat time series, Remote Sens. Environ, 207, 84–97, doi:10.1016/j.rse.2017.12.025, 2018.

Wang, W., Xiang, Y., Gao, Y., Lu, A. and Yao, T.: Rapid expansion of glacial lakes caused by climate and glacier retreat in the Central Himalayas, Hydrol. Process., 29, 859-874, 2014.

Wang, X., Chai, K., Liu, S., Wei, J., Jiang, Z., and Liu, Q.: Changes of glaciers and glacial lakes implying corridor-barrier effects and climate change in the Hengduan Shan, southeastern Tibetan Plateau, J. Glaciol., 63, 535-542, doi:10.1017/jog.2017.14, 2017.

Wang X., Guo X., Yang C., Liu Q., Wei J., Zhang Y., Liu S., Zhang Y., Jiang Z., and Tang Z.: Glacial lake inventory of High Mountain Asia, National Special Environment and Function of Observation and Research Stations Shared Service Platform, doi:10.12072/casnw.064.2019.db, 2019a.

Wang, X., Ding, Y., and Zhang, Y.: The influence of glacier meltwater on the hydrological effect of glacial lakes in mountain cryosphere, J. Lake Sci., 31, 609-620, 2019b.

Wang, X., Ding, Y., Liu, S., Jiang, L., Wu, K., Jiang, Z., and Guo, W.: Changes of glacial lakes and implications in Tian Shan, central Asia, based on remote sensing data from 1990 to 2010, Environ. Res. Lett. , 8, 044052, doi:10.1088/1748-9326/8/4/044052, 2013.

Wang X., Guo X., Yang C., Liu Q., Wei J., Zhang Y., Liu S., Zhang Y., Jiang Z., and Tang Z.: Glacial lake inventory of High Mountain Asia, National Special Environment and Function of Observation and Research Stations Shared Service Platform, doi:10.12072/casnw.064.2019.db, 2019a.

Wang, X., Liu, S., Guo, W., Yao, X., Jiang, Z., and Han, Y.: Using Remote Sensing Data to Quantify Changes in Glacial Lakes in the Chinese Himalaya, Mt. Res. Dev., 32, 203-212, doi: 10.1659/mrd-journal-d-11-00044.1, 2012.

Wang, X., Liu, Q., Liu, S., Wei, J., and Jiang, Z.: Heterogeneity of glacial lake expansion and its contrasting signals with climate change in Tarim Basin, Central Asia, Environ. Earth Sci., 75, 696, doi:10.1007/s12665-016-5498-4, 2016.

Worni, R., Huggel, C., and Stoffel, M.:Glacial lakes in the Indian Himalayas — From an area-wide glacial lake inventory to on-site and modeling based risk, Sci. Total Environ., 468-469, S71-84, doi:10.1016/j.scitotenv.2012.11.043, 2013.

Yang, C., Wang, X., Wei, J., Liu, Q., Lu, A., Zhang, Y., Tang, Z.: Chinese glacial lake inventory based on 3S technology method, J Geogr Sci, 74, 544-556, doi:10.11821/dlxb201903011, 2019.

Yao, X., Liu, S., Han, L., Sun, M., and Zhao, L.: Definition and classification system of glacial lake for inventory and hazards study, J. Geogr. Sci., 28, 193-205, 2018.

Yao, T., Thompson, L., Yang, W., Yu, W., Gao, Y., Guo, X., Yang, X., Duan, K., Zhao, H., and Xu, B.: Different glacier status with atmospheric circulations in Tibetan Plateau and surroundings, Nat. Clim. Chang, 2, 663–667, doi:10.1038/nclimate1580, 2012.

Zhai, K., Wu, X., Qin, Y., and Du, P.: Comparison of surface water extraction performances of different classic water indices using OLI and TM imageries in different situations, Geo-spatial Information Science, 18, 32-42, doi: 10.1080/10095020.2015.1017911, 2015.

Zhang, G., Bolch, T., Alien, S., Linsbauer, A., Chen, W., and Wang, W.: Glacial lake evolution and glacier–lake interactions in the Poiqu River basin, central Himalaya,1964–2017, J. Glaciol., 65 , 347–365, doi:10.1017/jog.2019.13, 2019.

Zhang, G., Yao, T., Xie, H., Wang, W., and Yang, W.: An inventory of glacial lakes in the Third Pole region and their changes in response to global warming, Glob. Planet. Change, 131, 148–157, doi: 10.1016/j.gloplacha.2015.05.01, 2015.

Zhang, M., Chen, F., and Tian, B. An automated method for glacial lake mapping in High Mountain Asia using Landsat 8 imagery. J. Mt. Sci. 15, 13-24, doi: 10.1007/s11629-017-4518-5, 2018.